J. Am. Soc. Mass Spectrom. (2013) 24:1603–1607
DOI: 10.1007/s13361-013-0703-0

RESEARCH ARTICLE

Cyanide–Arene Meisenheimer Complex Generated in Electrospray Ionization Mass Spectrometry Using Acetonitrile as a Solvent

Barbara Chiavarino,[1] Philippe Maitre,[2] Simonetta Fornarini,[1] Maria Elisa Crestoni[1]

[1]Dipartimento di Chimica e Tecnologie del Farmaco, Università degli Studi di Roma La Sapienza, P.le A. Moro 5, 00185 Rome, Italy
[2]Laboratoire de Chimie Physique, UMR8000 CNRS Faculté des Sciences, Université Paris Sud, Bâtiment 350, 91405 Orsay Cedex, France

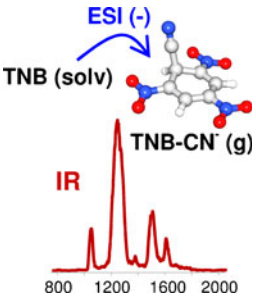

Abstract. The C – C bond formation activated under negative electrospray ionization of an acetonitrile solution of 1,3,5-trinitrobenzene is reported. The solvent function is to provide a source of cyanide ion, a highly problematic reagent, which is found to attack the electron-deficient aromatic ring to form a covalently bound anionic complex (Meisenheimer complex). The structure of the complex is elucidated by means of collision induced dissociation mass spectrometry and IR multiple photon dissociation spectroscopy in the 'fingerprint' region.

Key words: IRMPD spectroscopy, Meisenheimer complexes, C – C coupling, Tandem mass spectrometry, Ab initio calculations

Received: 14 May 2013/Revised: 8 July 2013/Accepted: 8 July 2013/Published online: 18 August 2013

Introduction

Cyanide ion is a valuable inorganic reagent forming C – C bonds with a variety of different substrates. However, its toxicity discourages using it in routine synthetic procedures such as the cyanation of aromatic compounds [1]. Several alternative cyanide sources have been utilized, including cuprous thiocyanate [2], ethylcyanoacetate [3], $K_4[Fe(CN)_6]$ [4], and benzyl cyanide [5]. Most of these methods require transition metal catalysis [6], though, and suffer from production of metal waste, poisoning of the catalyst and formation of toxic HCN. In this context, the smooth formation of a cyanide adduct of 1,3,5-trinitrobenzene (TNB), a strongly electron-deficient arene, upon electrospray ionization (ESI) of an acetonitrile solution in negative ion mode is a remarkable finding. The adduct is revealed at *m/z* 239 as the major ionic species (100 %) together with an ion at *m/z* 212 (20 %) corresponding to deprotonated TNB. The search for the cyanide adduct of TNB ($[TNB + CN]^-$) originates from our ongoing interest in the negatively charged adducts of simple, inorganic anions with π-acidic aromatic systems [7, 8]. Elucidating the structural features of $[TNB + CN]^-$ is the subject of the present contribution, exploiting collision induced dissociation experiments and infrared multiple photon dissociation (IRMPD) spectroscopy in the fingerprint region [9–15]. In addition, quantum chemical calculations were performed to sample candidate structures, providing optimized geometries, relative energies, and computed IR spectra.

Experimental

Minimum energy geometries and harmonic vibrational frequencies of candidate isomers were obtained by calculations performed at B3LYP/6-311 + G(d,p) level. Zero-point energy corrections were applied to the thermodynamic parameters (zero Kelvin). For a comparison to the experiment, computed vibrational frequencies were scaled by a factor of 0.99 and simulated IR spectra are obtained from a convolution with a Gaussian line shape of 20 cm^{-1} width.

Electronic supplementary material The online version of this article (doi:10.1007/s13361-013-0703-0) contains supplementary material, which is available to authorized users.

Correspondence to: Maria Elisa Crestoni; *e-mail:* mariaelisa.crestoni@uniroma1.it

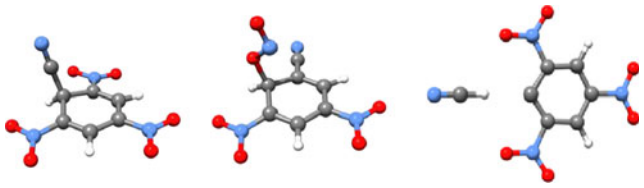

Figure 1. Optimized structures for [TNB + CN– complexes at B3LYP/6-311 + G(d,p) level. In parentheses, relative energies (kJ mol^{-1}) at 0 K

The gaseous ions were obtained using an electrospray ionization (ESI) source through direct infusion of a 0.3 mM solution of TNB (Sigma-Aldrich s.r.l. Milan, Italy) in acetonitrile using a syringe pump. CID experiments at variable energy were carried out using a 2000 Q Trap instrument (Applied Biosystems SCIEX, Concord, ON, Canada), a commercial hybrid triple quadrupole linear ion trap mass spectrometer ($Q1q2Q_{LIT}$). Typical ESI conditions were a flow rate of 3–5 μL/min, ion spray voltage at −4500 kV, declustering potential at −5 V, and entrance potential at −2 V. The ion of interest was mass-selected using Q1. CID experiments were performed in the quadrupole collision cell q2 at variable collision energies (E_{lab} = 5–35 eV) with N_2 as collision gas at a nominal pressure of 2.4–4.0 × 10^{-5} mbar. The dissociation product pattern was monitored by scanning Q_{LIT}.

IRMPD experiments were performed using a quadrupole ion trap instrument (Bruker Esquire 3000+) coupled to the beamline of the IR free electron laser (FEL) at the CLIO facility [16], as previously described [17–22]. Mass selected ions were irradiated with the FEL IR beam for 150 ms. For these experiments, the FEL was operated at 46 MeV and a fairly stable power of 900–1100 mW was ensured. The abundances of the parent and fragment ions were recorded as a function of the IR wave number to obtain the IR action spectra where the IRMPD efficiency (R) was plotted versus the photon energy [17–19].

Results and Discussion

The anionic σ-complex formed by addition of CN^- to an unsubstituted carbon of TNB (isomer **1** in Figure 1) is found to be a stable species. This species conforms to a Meisenheimer complex (the well-established intermediate of the S_NAr addition-elimination mechanism of nucleophilic aromatic substitution) stabilized by three nitro groups in ortho/para positions, effectively delocalizing the negative charge. The possible binding of cyanide to a nitro-substituted carbon has also been explored. However, the starting geometry evolves upon geometry optimization to isomer **2** (Figure 1), following C – NO_2 bond cleavage and binding to an adjacent carbon by an oxygen atom. Finally, the possibility that the ion at *m/z* 239 may rather correspond to a noncovalent species involving hydrogen bonding has been considered, yielding a complex of deprotonated TNB ($[TNB – H]^-$) interacting with HCN (**3** in Figure 1), in line with the comparatively higher basicity of cyanide relative to $[TNB – H]^-$. The optimized geometries of **1**–**3** are given in Table S1 as Online Resource and the relative energies of **1**–**3** and of related species are given in Table 1.

Species **1** and **2** are very close in energy. However, their dissociation behavior is expected to be quite different. Cyanide cleavage from **1** should lead to HCN and deprotonated

Table 1. Absolute Electronic Energies, Zero Point Energies (ZPE), and Relative Energies at 0 K of $[TNB + CN]^-$ Complexes **1**–**3** and of Related Species. Computations at B3LYP/6-311 + G(d,p) Level

Species	E(hartree)	ZPE(kJ mol^{-1})	E_{rel}(kJ mol^{-1})	nimag[a]
$[TNB + CN]^-$ (**1**)	−938.958618	303	0	0
$[TNB + CN]^-$ (**2**)	−938.959390	298	−7	0
$[TNB + CN]^-$ (**3**)	−938.903196	289	131	0
$TNB + CN^-$	−938.871474	292	218	
$[TNB - H]^- + HCN$	−938.877719	285	194	
$CN - DNB^b + NO_2^-$	−938.912915	291	108	
$[CN - DNB - H]^{-b} + HNO_2$	−938.894670	286	151	
CN^- [c]	−92.8884767	13		0
HCN[c]	−93.4545134	43		0
TNB[d]	−845.982997	279		0
$[TNB - H]^-$ [d]	−845.423206	242		0
$CN - DNB^{b,e}$	−733.687905	270		0
$[CN - DNB - H]^-$ [b,e]	−733.122858	233		0
NO_2^- [f]	−205.225010	21		0
HNO_2[f]	–205.771780	53		0

[a]nimag is number of imaginary frequencies
[b]CN - DNB is 3,5-dinitrobenzonitrile
[c]These data point to $\Delta H°_{acid}$ of HCN equal to 1456 kJ mol^{-1} at 0 K
[d]These data point to $\Delta H°_{acid}$ of TNB equal to 1432 kJ mol^{-1} at 0 K
[e]These data point to $\Delta H°_{acid}$ of CN - DNB equal to 1446 kJ mol^{-1} at 0 K
[f]These data point to $\Delta H°_{acid}$ of HNO_2 equal to 1403 kJ mol^{-1} at 0 K

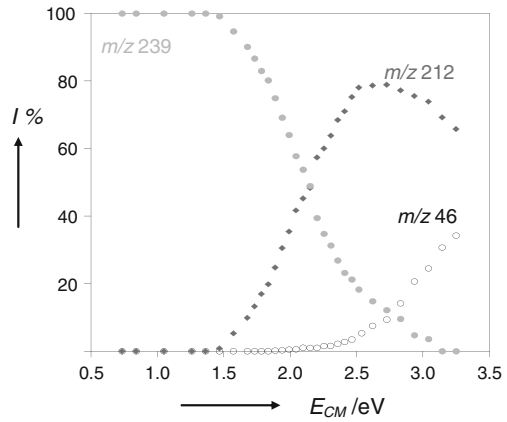

Figure 2. Relative abundances of parent (*m/z* 239) and fragment ions (*m/z* 212 and 46) as a function of the translational energy in the center of mass frame

TNB (Equation (1)) in a process endothermic by 194 kJ mol^{-1}. Isomer **3** may be an intermediate in the dissociation reaction.

$$\mathbf{1} \rightarrow [\mathrm{TNB} - \mathrm{H}]^- + \mathrm{HCN} \quad (1)$$

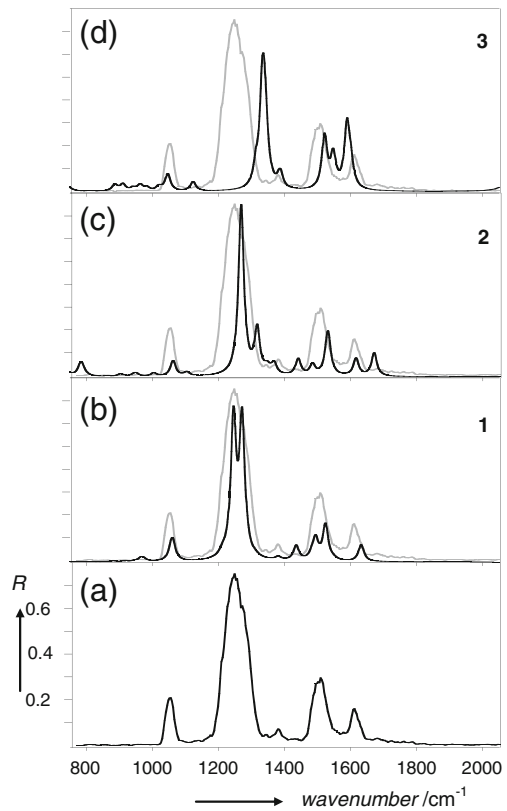

Figure 3. IRMPD spectrum of $[TNB + CN]^-$ **(a)** and comparison with calculated IR spectra of **1–3 (b)–(d)**, respectively

Conversely, the dissociation of **2** into NO_2^- and 3,5-dinitrobenzonitrile is endothermic by 108 kJ mol^{-1}. In order to ascertain the fragmentation behaviour of the sample ions at *m/z* 239, collision induced dissociation experiments at variable energy have been performed in a hybrid QqTrap instrument (Figure 2).

The ions, selected in the first sector and submitted to collisions with dinitrogen at increasing center of mass energy (E_{CM}) in the second quadrupole, display fragment ions at *m/z* 212 ($[TNB - H]^-$) and *m/z* 46 (NO_2^-). However, the former species is the only ion formed at the lowest collision energies, nitrite ion appearing at considerably higher collision energy in spite of a comparatively much lower endothermicity for the dissociation process depicted in Equation (2), (Table 1).

$$\mathbf{2} \rightarrow NO_2^- + 3,5\text{-dinitrobenzonitrile} \quad (2)$$

The CID evidence suggests **1** as the structure of the $[TNB + CN]^-$ sampled ions, formed by the direct attack of cyanide to the ring position activated by the ortho/para nitro groups. Further support for the structural assignment was obtained by IRMPD spectroscopy using the IR radiation of a FEL tuned in the mid-IR region at the CLIO (Centre Laser Infra Rouge d'Orsay) center coupled with a Paul type ion trap mass spectrometer [16, 23]. The IRMPD spectrum is obtained by reporting the photofragmentation yield as a function of the radiation wavenumber.

Photons in resonance with active vibrational modes promote fragmentation of $[TNB + CN]^-$ to give $[TNB - H]^-$ and HCN, namely the same products observed under CID at relatively low collision energy. It is generally recognized that IR multiple photon absorption provides a slow heating process leading to the photofragment associated with the lowest energy fragmentation threshold [10]. A sizeable activation barrier is clearly involved in the dissociation to NO_2^- that is observed under CID

Table 2. Assignment of IRMPD Bands for $[TNB + CN]^-$ Compared with Calculated IR Transitions (B3LYP/6-311 + G(d,p) Level)

Experimental IRMPD[a]	Calculated IR[a,b]	Vibrational mode
1050	1057 (185)	CH bending (in plane)
	1063 (159)	CH bending (in plane)
1244	1245 (1876)	NO_2 symm stretch, C – N stretch
1275	1272 (1867)	NO_2 symm stretch, C – N stretch
1380	1381 (96)	Ring def, C – N stretch
1504	1494 (279)	NO_2 asymm stretch
	1524 (485)	NO_2 asymm stretch, C – C stretch
1610	1632 (227)	C – C stretch

[a]Frequency in cm^{-1}
[b]Intensity (in parentheses) in km/mol

at relatively high collision energy, although the process is thermodynamically less demanding. The IRMPD spectrum is shown in Figure 3a, presenting also the calculated IR spectra for the candidate isomers **1**–**3** (Figure 3b–d). The experimental spectrum drawn in grey in Figure 3b–d shows that the best agreement is observed with the calculated IR spectrum of **1**. The match between the experimental features and the calculated IR transitions is also clear in the corresponding data listed in Table 2. The dominant band at 1244 cm^{-1} with a barely discernible shoulder at 1275 cm^{-1} is associated to NO_2 symmetric stretching and CN stretching vibrations involving the nitro substituents. In plane CH bending modes are responsible for the IRMPD band at 1050 cm^{-1}. A pronounced band at 1504 cm^{-1} comprises NO_2 symmetric stretching modes and a somewhat weaker one at 1610 cm^{-1} is associated to C – C stretching vibration. A small feature at 1380 cm^{-1} in the IRMPD spectrum matches the transition at 1381 cm^{-1} associated to ring deformation and C–N stretching. A comparatively more active mode expected at 1435 cm^{-1} is instead not observed experimentally. It has been previously observed that small absorptions may be missing in IRMPD spectra [11, 24–29]. Possible reasons lie in the multiphotonic nature of IRMPD and in the demand of efficient intramolecular vibrational relaxation.

The major band at 1244 cm^{-1} involving stretching vibrations of the nitro groups is a characteristic feature of the anionic σ-complex structure. These modes are degenerate and resonant at higher frequency in neutral TNB. In the anionic σ-complex the three nitro groups become nonequivalent and degeneracy is removed. The symmetric stretching of the para nitro group contributes mainly to the transition predicted at 1272 cm^{-1} whereas the ortho ones are mainly active at 1245 cm^{-1}. The separation of the two transitions, hardly resolved in the experimental IRMPD spectrum, and their notable activity account for the remarkable bandwidth (90 cm^{-1} width at half maximum). The red shift with respect to neutral TNB originates from the resonance interaction of the nitro groups in the anionic σ-complex, leading to a diminished N – O bond order. These features have already been pointed out in the IRMPD spectroscopic study of exemplary adducts of simple anions with TNB, presenting evidence of two types of structural motifs [8], namely a weakly covalent σ interaction and a strongly covalent σ interaction [30]. The exceptionally large bandwidth of the dominant feature in the IRMPD spectrum is well accounted for by the two transitions of comparable activity in the calculated IR spectrum of isomer **1**. The IR spectrum of isomer **2** does not support this feature, though presenting also a general fair agreement. Isomer **2**, if present in the sampled ion is, however, expected to yield the **2** → NO_2^- + 3,5-dinitrobenzonitrile fragmentation path, which is not detected under IRMPD conditions.

Overall, the gathered evidence provides strong indication for the anionic σ-complex **1** to be the structure of ESI-formed $[TNB + CN]^-$ ions.

Conclusion

In a recent communication [31], electrosonically generated droplets have been found to allow a medium enhancing the rate of C – C bond forming reactions. This novel result, providing a preparative electrospray process, is explained to arise from a concentration effect. Reactant concentration increases in the shrinking droplet, increasing the rate of the bimolecular reaction. In contrast, the CN^- donating ability of the acetonitrile solvent under the adopted negative ESI conditions likely stems from the character of a special electrolytic cell associated to the ESI device [32]. This reactivity behavior has provided a neat route to the adduct of CN^- with an exemplary π-acidic arene, characterized as an anionic σ–complex in an isolated state. In an interesting previous report, cyanide adducts of 1,3,5-trinitrobenzene and 2,4,6-trinitrotoluene have been revealed in the course of atmospheric pressure chemical ionization and desorption atmospheric pressure chemical ionization. Their fragmentation patterns upon collisional activation were found to be consistent with the structure of Meisenheimer complexes [33]. The covalent structure of the sampled $[TNB + CN]^-$ ions is in line with the high basicity of cyanide [30]. In summary, the gas-phase chemistry of anionic σ–complexes (Meisenheimer complexes) reveals increasingly interesting facets [34–40].

Acknowledgments

The authors acknowledge funding for this work by the Italian MIUR (PRIN project no. 2009W2W4YF_004) and by the European Community's Seventh Framework Programme (FP7/2007-2013, under grant agreement no 226716). The authors are grateful to J. M. Ortega, D. Scuderi, J. Lemaire, and to the CLIO team for their supportive assistance.

Dedicated to the memory of Professor Fulvio Cacace, mentor and friend, on the 10th anniversary of his untimely demise.

References

1. Anbarasan, P., Schareina, T., Beller, M.: Recent developments and perspectives in palladium-catalyzed cyanation of aryl halides: synthesis of benzonitriles. *Chem. Soc. Rev.* **40**, 5049–5067 (2011)
2. Zhang, G.-Y., Yu, J.-T., Hu, M.-L., Cheng, J.: Palladium-catalyzed cyanation of aryl halides with CuSCN. *J. Org. Chem.* **78**, 2710–2714 (2013)

3. Zheng, S., Yu, C., Shen, Z.: Ethyl cyanoacetate: a new cyanating agent for the palladium-catalyzed cyanation of aryl halides. *Org. Lett.* **14**, 3644–3647 (2012)
4. Yeung, P.Y., Tsang, C.P., Kwong, F.Y.: Efficient cyanation of aryl bromides with $K_4[Fe(CN)_6]$ catalyzed by a palladium-indolylphosphine complex. *Tetrahedron Lett.* **52**, 7038–7041 (2011)
5. Wen, Q., Jin, J., Hu, B., Lu, P., Wang, Y.: Palladium-catalyzed cyanide metathesis: utilization of benzyl cyanide as an operator-benign reagent for aryl halide cyanations. *RSC Adv.* **2**, 6167–6169 (2012)
6. Kim, J., Kim, H.J., Chang, S.: Synthesis of aromatic nitriles using nonmetallic cyano-group sources. *Angew. Chem. Int. Ed.* **51**, 11948–11959 (2012)
7. Chiavarino, B., Crestoni, M.E., Fornarini, S., Lanucara, F., Lemaire, J., Maitre, P.: Meisenheimer complexes positively characterized as stable intermediates in the gas phase. *Angew. Chem. Int. Ed.* **46**, 1995–1998 (2007)
8. Chiavarino, B., Crestoni, M.E., Fornarini, S., Lanucara, F., Lemaire, J., Maitre, P., Scuderi, D.: Molecular complexes of simple anions with electron-deficient arenes: spectroscopic evidence for two types of structural motifs for anion-arene interactions. *Chem. Eur. J.* **15**, 8185–8195 (2009)
9. Oomens, J., Sartakov, B.G., Meijer, G., von Helden, G.: Gas-phase infrared multiple photon dissociation spectroscopy of mass-selected molecular ions. *Int. J. Mass Spectrom.* **254**, 1–19 (2006)
10. MacAleese, L., Maitre, P.: Infrared spectroscopy of organometallic ions in the gas phase: from model to real world complexes. *Mass Spectrom. Rev.* **26**, 583–605 (2007)
11. Eyler, J.R.: Infrared multiple photon dissociation spectroscopy of ions in Penning traps. *Mass Spectrom. Rev.* **28**, 448–467 (2009)
12. Fridgen, T.D.: Infrared consequence spectroscopy of gaseous protonated and metal ion cationized complexes. *Mass Spectrom. Rev.* **28**, 586–607 (2009)
13. Polfer, N.C.: Infrared multiple photon dissociation spectroscopy of trapped ions. *Chem. Soc. Rev.* **40**, 2211–2221 (2011)
14. Duncan, M.A.: Infrared laser spectroscopy of mass-selected carbocations. *J. Phys. Chem. A* **116**, 11477–11491 (2012)
15. Roithova, J.: Characterization of reaction intermediates by ion spectroscopy. *Chem. Soc. Rev.* **41**, 547–559 (2012)
16. MacAleese, L., Simon, A., McMahon, T.B., Ortega, J.-M., Scuderi, D., Lemaire, J., Maitre, P.: Mid-IR spectroscopy of protonated leucine methyl ester performed with an FTICR or a Paul type ion-trap. *Int. J. Mass Spectrom.* **249/250**, 14–20 (2006)
17. Chiavarino, B., Crestoni, M.E., Fornarini, S., Lanucara, F., Lemaire, J., Maitre, P., Scuderi, D.: Infrared spectroscopy of isolated nucleotides. 1. The cyclic 3′,5′-adenosine monophosphate anion. *Int. J. Mass Spectrom.* **270**, 111–117 (2008)
18. Chiavarino, B., Crestoni, M.E., Fornarini, S., Taioli, S., Mancini, I., Tosi, P.: Infrared spectroscopy of copper-resveratrol complexes: a joint experimental and theoretical study. *J. Chem. Phys.* **37**(2), 024301–024309 (2012)
19. Lanucara, F., Chiavarino, B., Crestoni, M.E., Scuderi, D., Sinha, R.K., Maitre, P., Fornarini, S.: Naked five-coordinate FeIII(NO) porphyrin complexes: vibrational and reactivity features. *Inorg. Chem.* **50**, 4445–4452 (2011)
20. Chiavarino, B., Crestoni, M.E., Fornarini, S., Dopfer, O., Lemaire, J., Maitre, P.: IR spectroscopic features of gaseous $C_7H_7O^+$ ions: benzylium versus tropylium ion structures. *J. Phys. Chem. A* **110**, 9352–9360 (2006)
21. Chiavarino, B., Crestoni, M.E., Fornarini, S., Lemaire, J., Maitre, P., MacAleese, L.: π-complex structure of gaseous benzene-NO cations assayed by IR multiple photon dissociation spectroscopy. *J. Am. Chem. Soc.* **128**, 12553–12561 (2006)
22. Lorenz, U.J., Lemaire, J., Maitre, P., Crestoni, M.-E., Fornarini, S., Dopfer, O.: Protonation of heterocyclic aromatic molecules: IR signature of the protonation site of furan and pyrrole. *Int. J. Mass Spectrom.* **267**, 43–53 (2007)
23. Simon, A., MacAleese, L., Maitre, P., Lemaire, J., McMahon, T.B.: Fingerprint vibrational spectra of protonated methyl esters of amino acids in the gas phase. *J. Am. Chem. Soc.* **129**, 2829–2840 (2007)
24. Sinha, R.K., Chiavarino, B., Fornarini, S., Lemaire, J., Maitre, P., Crestoni, M.E.: Protonated sulfuric acid: vibrational signatures of the naked ion in the near- and mid-IR. *J. Phys. Chem. Lett.* **1**, 1721–1724 (2010)
25. Moore, D.T., Oomens, J., Eyler, J.R., von, H.G., Meijer, G., Dunbar, R.C.: Infrared spectroscopy of gas-phase Cr+ coordination complexes: determination of binding sites and electronic states. *J. Am. Chem. Soc.* **127**, 7243–7254 (2005)
26. Schroeder, D., Schwarz, H., Milko, P., Roithova, J.: Dissociation routes of protonated toluene probed by infrared spectroscopy in the gas phase. *J. Phys. Chem. A* **110**, 8346–8353 (2006)
27. Chiavarino, B., Crestoni, M.E., Fornarini, S., Lemaire, J., MacAleese, L., Maitre, P.: Infrared spectroscopy of protonated phenylsilane in the gas phase. *Chem. Phys. Chem.* **6**, 437–440 (2005)
28. Chiavarino, B., Crestoni, M.E., Dopfer, O., Maitre, P., Fornarini, S.: Benzylium versus tropylium ion dichotomy: vibrational spectroscopy of gaseous $C_8H_9^+$ ions. *Angew. Chem. Int. Ed.* **51**, 4947–4949 (2012)
29. Chiavarino, B., Crestoni, M.E., Fornarini, S., Scuderi, D., Salpin, J.-Y.: interaction of cisplatin with adenine and guanine: a combined irmpd, MS/MS, and Theoretical Study. *J. Am. Chem. Soc.* **135**, 1445–1455 (2013)
30. Hay, B.P., Bryantsev, V.S.: Anion-arene adducts: C–H hydrogen bonding, anion-π interaction, and carbon bonding motifs. *Chem. Commun.* 2417–2428 (2008)
31. Mueller, T., Badu-Tawiah, A., Cooks, R.G.: Accelerated carbon[n.63743]Carbon bond-forming reactions in preparative electrospray. *Angew. Chem. Int. Ed.* **51**, 11832–11835 (2012)
32. Kebarle, P., Verkerk, U.H.: Electrospray: from ions in solution to ions in the gas phase, what we know now. *Mass Spectrom. Rev.* **28**, 898–917 (2009)
33. Song, Y., Cooks, R.G.: Atmospheric pressure ion/molecule reactions for the selective detection of nitroaromatic explosive using acetonitrile and air as reagents. *Rapid Commun. Mass Spectrom.* **20**, 3130–3138 (2006)
34. Dillow, G.W., Kebarle, P.: Fluoride affinities of perfluorobenzenes C_6F_5X. Meisenheimer complexes in the gas phase and solution. *J. Am. Chem. Soc.* **110**, 4877–4882 (1988)
35. Chen, H., Chen, H., Cooks, R.G.: Meisenheimer complexes bonded at carbon and at oxygen. *J. Am. Soc. Mass Spectrom.* **15**, 998–1004 (2004)
36. Giroldo, T., Xavier, L.A., Riveros, J.M.: An unusually fast nucleophilic aromatic displacement reaction: the gas-phase reaction of fluoride ions with nitrobenzene. *Angew. Chem. Int. Ed.* **43**, 3588–3590 (2004)
37. Fernandez, I., Frenking, G., Uggerud, E.: Rate-determining factors in nucleophilic aromatic substitution reactions. *J. Org. Chem.* **75**, 2971–2980 (2010)
38. Garver, J.M., Yang, Z., Kato, S., Wren, S.W., Vogelhuber, K.M., Lineberger, W.C., Bierbaum, V.M.: Gas phase reactions of 1,3,5-triazine: proton transfer, hydride transfer, and anionic σ-adduct formation. *J. Am. Soc. Mass Spectrom.* **22**, 1260–1272 (2011)
39. Danikiewicz, W., Bienkowski, T., Poddebniak, D.: Generation and reactions of anionic σ-adducts of 1,3-dinitrobenzene and 1,3,5-trinitrobenzene with carbanions in a gas phase, using an electrospray ion source as the chemical reactor. *J. Am. Soc. Mass Spectrom.* **15**, 927–933 (2004)
40. Danikiewicz, W., Bienkowski, T., Wojciechowski, K.: Application of electrospray ionization mass spectrometry for studies of anionic σ-adducts of aromatic nitro-compounds. *Tetrahedron Lett.* **45**, 931–934 (2004)